



A female head–neck model for rear impact simulations



Jonas Östh ^{a,*}, Manuel Mendoza-Vazquez ^a, Fusako Sato ^{a,b}, Mats Y. Svensson ^a,
Astrid Linder ^{a,c}, Karin Brodin ^a

^a Department of Applied Mechanics, Chalmers University of Technology, SE – 412 96 Gothenburg, Sweden

^b Japan Automobile Research Institute, Tsukuba, Ibaraki, Japan

^c Statens väg- och transportforskningsinstitut (VTI), Box 8072, SE – 402 78 Gothenburg, Sweden

ARTICLE INFO

Article history:

Accepted 26 November 2016

Keywords:

Female
Finite element
Human body model
Rear impact
Whiplash

ABSTRACT

Several mathematical cervical models of the 50th percentile male have been developed and used for impact biomechanics research. However, for the 50th percentile female no similar modelling efforts have been made, despite females being subject to a higher risk of soft tissue neck injuries. This is a limitation for the development of automotive protective systems addressing Whiplash Associated Disorders (WADs), most commonly caused in rear impacts, as the risk for females sustaining WAD symptoms is double that of males.

In this study, a finite element head and neck model of a 50th percentile female was validated in rear impacts. A previously validated ligamentous cervical spine model was complemented with a rigid body head, soft tissues and muscles. In both physiological flexion–extension motions and simulated rear impacts, the kinematic response at segment level was comparable to that of human subjects. Evaluation of ligament stress levels in simulations with varied initial cervical curvature revealed that if an individual assumes a more lordotic posture than the neutral, a higher risk of WAD might occur in rear impact.

The female head and neck model, together with a kinematical whole body model which is under development, addresses a need for tools for assessment of automotive protection systems for the group which is at the highest risk to sustain WAD.

© 2016 The Authors. Published by Elsevier Ltd. This is an open access article under the CC BY-NC-ND license (<http://creativecommons.org/licenses/by-nc-nd/4.0/>).

1. Introduction

Finite Element (FE) Human Body Models (HBMs) are important tools for investigating the human response to impact loads; e.g. [Stemper et al. \(2005\)](#) studied the effect of having a lordotic, straight, or kyphotic neutral curvature of the cervical spine in rear impact. Their model is one of several cervical spine models of the 50th percentile male ([de Bruijn et al., 2015](#); [de Jager, 1996](#); [Ejima et al., 2005](#); [Halldin et al., 2000](#); [Kitagawa et al., 2008](#); [Mustafy et al., 2014](#); [Nightingale et al., 2016](#); [Panzer and Cronin, 2009](#); [Yang et al., 1998](#)). Presently, similar efforts for the 50th percentile female have not been made ([Brolin et al., 2015](#)), which limit the development of automotive protection systems addressing neck injuries for which the prevalence is affected by the gender of the crash victim.

Gender has been shown to be an important factor for the risk of sustaining Whiplash Associated Disorders (WAD); the risk for females sustaining symptoms is on average double that of males

and in similar crash conditions even higher ([Carstensen et al., 2012](#); [Jakobsson et al., 2004](#); [Krafft et al., 2003](#); [Morris and Thomas, 1996](#); [O'Neill et al., 1972](#); [Temming and Zobel, 1998](#)). WAD can occur in all impact directions, with rear impacts occurring most frequently in accident statistics ([Stigson et al., 2015](#); [Watanabe et al., 2000](#)). WADs originate from damage to the soft tissue structures of the neck and a significant part of long term disability resulting from vehicle crashes is caused by WAD, up to 70% in Sweden ([Kullgren et al., 2007](#)). In particular, so called S-shaped deformation of the cervical spine during rear impact is considered pivotal for the mechanism causing WAD ([Stemper et al., 2005](#)); it has been reported for both volunteers and PMHS in rear impacts ([Kaneoka et al., 1999](#); [Stemper et al., 2003](#); [Yoganandan et al., 2000](#)).

There are several systematic morphological differences between female and male cervical spines ([Stemper et al., 2011](#)). For instance the circumference of the female cervical spine relative to the length of the neck is smaller, as is the vertebral body sizes, and it has 20–32% less muscle strength for size matched subjects ([Vasavada et al., 2008](#)). Hence, scaling of existing male models to female size has been proven inadequate ([Mordaka, 2004](#)). In addition, [Sato et al. \(2016\)](#) recently showed that male and female volunteers exhibit different alignment patterns of the whole spine

* Corresponding author.

E-mail addresses: jonas.osth@chalmers.se (J. Östh), manuel.mendoza-vazquez@chalmers.se (M. Mendoza-Vazquez), fusako.sato@chalmers.se (F. Sato), mats.svensson@chalmers.se (M.Y. Svensson), astrid.linder@vti.se (A. Linder), karin.brolin@chalmers.se (K. Brodin).

in the same seat, which could also influence the outcome of a rear impact.

The availability of a validated, detailed female FE model of the cervical spine for impact would aid the development of in-vehicle protective systems for the group at the highest risk to sustain an injury which causes significant suffering and economic loss. Therefore, the aim of this study was to validate a 50th percentile female head–neck model in rear impacts and to investigate the influence of different spinal curvatures for the same individual on the kinematic and mechanical parameters associated with WAD.

2. Method

For this study, a previously developed ligamentous cervical spine model (Östh et al., 2016a, 2016b) was complemented with a skull and soft tissues to create the head–neck model, Fig. 1. The skull and soft tissues were created from the stereolithography (STL) surfaces of the skeleton and outer surface of a 31 year old female subject of 161.6 cm stature and 60.8 kg weight, within 0.1% and 2% from the target 50th percentile female as defined by Schneider et al. (1983). In addition, ten more anthropometric measurements (e.g., seated height and hip breadth) were verified to be within 5% of the value for the 50th percentile female reported by Gordon et al. (1988). A total of 138 scan series with approximately 20,000 images were captured in an automotive seated posture using several modalities (magnetic resonance imaging, computed tomography, and external measurements) and processed to STL surfaces as described by Gayzik et al. (2009, 2011). Soft tissues for the head–neck model were generated based on the skeletal geometry, outer surface, and anatomical literature descriptions, while the skeleton was meshed directly from the STL surfaces.

Mesh generation was made with Hypermesh 13.0 (Altair, Troy, MI), simulations were run with single precision LS-DYNA MPP R8.1.1 (LSTC, Livermore, CA), and pre- and post-processing with LS-PrePost (LSTC, Livermore, CA) and Matlab (The Mathworks, Natick, MA). The developed model is released and distributed under an Open Source license, and is available for downloading from: <http://www.chalmers.se/en/projects/Pages/OpenHBM.aspx>.

A global coordinate system with X forward, Y to the left and Z upwards was utilised, Fig. 1. For all conducted simulations, gravity loading (a volume load of 9.81 m/s^2 in negative Z-direction) was included. The distal ends of muscles that attach to the shoulder girdle, lower thoracic vertebrae, and the costae, along with the free end of the cervical soft tissues, Fig. 1, was constrained to move with the T1 vertebral body. For some simulation results, objective rating criteria values (in the range of 0–1, e.g., cHX for correlation of head X-displacements) were calculated to compare model results with experimental data, using the weighted integration factor method (Hovenga et al., 2005).

2.1. Head model development

The head was modelled as a rigid body, Fig. 1, connected to the cervical spine by the atlantocranial ligaments, a sliding contact between the occipital condyles

and atlas, and by the continuous mesh of the external soft tissues. The head centre of mass was positioned in the midsagittal plane, at $X_a=0.2 \text{ mm}$ and $Z_a=29.1 \text{ mm}$ (the average for seven female Post Mortem Human Subjects (PMHSs) (Plaga et al., 2005; Yoganandan et al., 2009)) in the head anatomical coordinate system, Fig. 1. The principal axes of inertia were positioned at -34° rotation relative to the anatomical coordinate system (the average for 21 male and female PMHSs (Beier et al., 1980)). The mass of the head was set to 3.58 kg, equalling the EvaRID virtual rear impact dummy of a 50th female (Carlsson et al., 2014). Principal moments of inertia for the head rigid body was determined by regression equations (Plaga et al., 2005) to $I_{xx}=0.0151 \text{ kgm}^2$, $I_{yy}=0.0164 \text{ kgm}^2$, $I_{zz}=0.0109 \text{ kgm}^2$.

2.2. Cervical spine model development

The ligamentous cervical spine consists of approximately 116,000 elements; cortical bone is modelled with triangular shell elements, trabecular bone with tetrahedral elements, ligaments with orthotropic membrane elements, and intervertebral discs as composites of hexahedral elements and orthotropic quadrilateral membrane elements. It is described in detail and was validated for quasi-static loads in Östh et al. (2016a, 2016b). The material models of the lower cervical spine ligaments, calibrated in Östh et al. (2016a) with respect to quasi-static in vitro test data (Mattucci and Cronin, 2015), were complemented with a strain-hardening response (linear interpolation between quasi-static, 20/s, and 150–250/s strain-rates as reported by Mattucci and Cronin, 2015). Then, the skin of the head–neck model was represented by elastic quadrilateral membrane elements. The volume between the skin and spine was filled with hexahedral elements representing the soft tissues; the ligamentous spine interacts with the soft tissues by frictionless contact. The trachea cavity was modelled as an oval tube with an anteroposterior diameter of 19 mm and transverse diameter of 16 mm (Karmakar et al., 2014). It spans from the oral cavity, via the hyoid bone to the T1 level. From the hyoid bone to the fifth cervical vertebrae (C5) level (Burdett and Mitchell, 2008; Standring, 2008), the larynx was modelled with quadrilateral shell elements surrounding the trachea. Inferior to the larynx, three segments of tracheal cartilage are modelled with beam elements, partially surrounding the trachea (Burdett and Mitchell, 2008; Standring, 2008). The hyoid bone is modeled as a rigid body, connected to the cervical soft tissues and the stylohyoid ligament. Material data for the soft tissues are presented in Table 1.

Detailed data for the cervical spine muscles are available in a few dissection studies (Borst et al., 2011; Kamibayashi and Richmond, 1998; Van Ee et al., 2000); however, none of these are of a 50th percentile female. Of these studies, the most complete data set was presented by Borst et al. (2011), who reported origin and insertion points, Physiological Cross Sectional Areas (PCSAs), and tendon length data for 34 cervical muscles from an approximately 50th percentile male (171 cm stature, 75 kg weight, 86 years old). This data has two limitations for the present work with a 50th percentile female. First, as shown by Van Ee et al. (2000), healthy young subjects on average have 64% larger PCSA compared to PMHS. Second, PCSAs are on average 70% larger for males than for females (Marras et al. 2001). As these scaling factors cancel out, no scaling was done and cervical muscles were added to the HBM according to Borst et al. (2011) and anatomical descriptions (Standring 2008). All 129 fascicles except the omohyoid venter superior, thyrohyoid, and intercostalis cervicis fascicles were implemented bilaterally with one dimensional Hill-type elements, see Appendix A and Table 1, spanning from origin to insertion. For the fascicles of some muscles; the levator scapulae, longus colli, semispinalis

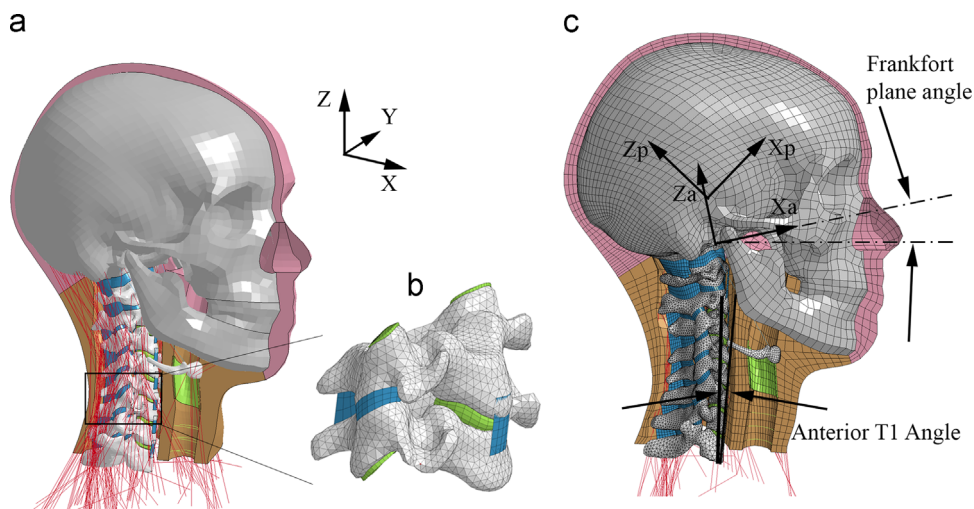


Fig. 1. (a): Overview of the head and neck of the female model and the global coordinate system used. (b): Close-up view of a sample vertebral segment (C5C6). (c) Sagittal plane view of the head–neck model with the head anatomical coordinate system (X_a – Z_a), the head principal axes of inertia (X_p – Z_p) which has its origin at the head centre of mass, the angle of the anterior surface of T1, and the Frankfort plane angle. The head rigid body includes the pink and grey structures in (a). (For interpretation of the references to color in this figure legend, the reader is referred to the web version of this article.)

Table 1

Summary of material and element properties used for the head-neck model. N/A = Not Applicable; Min. = Minimum; Max. = Maximum; LS-DYNA specific entries: ELFORM = element formulation number; HGID = hourglass formulation number; *MAT_no = material number.

Part(s)	Element type (ELFORM)	Characteristic element length (mm)	Hourglass control (HGID)	Constitutive model (*MAT_no)	Material parameters	Shell/beam thickness (mm)	References
Cervical soft tissues	Hexahedral (1)	Min.=1.1 Median=2.9 Max.=15.5	Stiffness based (5)	Ogden rubber (77_0)	$\rho=890 \text{ kg/m}^3$ $\nu=0.4999$ $\mu_1=30 \text{ Pa}$ $\alpha_1=20$ $G_1=3 \text{ kPa}$ $B_1=310 \text{ s}^{-1}$	N/A	Engelbrektsson (2011)
Skin	Quadrilateral membrane (9)	Min.=1.2 Median=3.1 Max.=14.7	N/A	Linear elastic (001)	$E=1 \text{ MPa}$ $\nu=0.40$	1 mm	Manschot and Brakkee (1988)
Larynx	Quadrilateral shell (2)	Min.=0.9 Median=2.0 Max.=6.6	Viscous (3)	Linear elastic (001)	$E=9.1 \text{ Mpa}$ $\nu=0.40$	2 mm	Roberts et al. (1998)
Tracheal cartilage	Beam (1)	Min.=1.0 Median=1.8 Max.=3.3	N/A	Linear elastic (001)	$E=9.1 \text{ Mpa}$ $\nu=0.40$	1 mm	Roberts et al. (1998)
Stylohyoid ligament	Beam(Cable) (6)	79.3	N/A	Linear elastic cable (071)	$E=1.2 \text{ Gpa}$	2 mm	Zajac (1989)
Cervical muscles	Beam (Resultant truss) (3)	Min.=10.4 Median=73.5 Max.=182.1	N/A	Hill muscle (156)	Maximum isometric stress $\sigma_m=0.5 \text{ Mpa}$ Shape of force-length relation $C_{sh}=0.225^*$ Maximum shortening velocity $V_{max}=4I_{opt}^*$ Shape of force-velocity relation $C_{short}=0.25$ $C_{mvi}=1.5$ $C_{leng}=0.1$ Shape of passive elastic relation $C_{pe}=6.0$ $PE_{max}=0.375^*$		Borst et al. (2011) Winters and Stark (1988) Walker and Schrodt (1974) Zajac (1989) Cole et al. (1996); van der Horst (2002); Östh et al. (2012); de Bruijn et al. (2015) Yamada (1970); Östh et al. (2012)

* C_{sh} , V_{max} , and PE_{max} were divided by 2 to compensate for muscles lengths being approximately 200% of physiological length.

capitis, splenius capitis and cervicis, and multifidus, the fascicles were split into more elements using the LS-DYNA card *PART_AVERAGED, and redirected at intermediate vertebrae to better follow the curvature of the spine. Similarly, the infrahyoid muscles were redirected at the hyoid bone and extended to the attachments of the suprahyoid muscles, i.e. one muscle with two or more elements was representing both an infra and suprahyoid. Tendon length was only available for minority of the fascicles reported (Borst et al., 2011); hence, tendons were omitted for all fascicles which lead to the optimal muscle lengths in the model being approximately 200% of the physiological length. To compensate, the shape factor for the force-length relation fitted to single sarcomere data for human muscle (Walker and Schrodt, 1974), the maximum shortening velocity (Zajac, 1989), and the passive elastic stiffness (Östh et al., 2012; Yamada, 1970) was divided by two, Table 1.

2.3. Spinal alignment assessment

The alignment of the cervical spine in the modelled posture, Fig. 1, was compared with volunteers in the study by Sato et al. (2016). Eight female volunteers (average stature and weight: 161 cm and 52 kg) were seated on a wooden seat with a 20° seat back angle and 10° seat pan angle, and instructed to face forward and be relaxed. The spinal curvature was presented for the geometrical centres of the vertebral bodies, including coordinates normalised by the length of the spine. In addition, the spinal curvature was assessed in accordance with Klinich et al. (2004); the curvature index was calculated using the midpoint of the inferior vertebral surface from C2 to C7, while Bezier angles were calculated using posterior landmarks on the vertebrae.

2.4. Strength evaluation

Maximal cervical flexion and extension strength was evaluated in two simulations with a duration of 1 s, with muscle activation linearly increased from 0 to 100% over the first 0.5 s. The ventral cervical muscles were activated as flexors, and the dorsal as extensors. In extension, for the dorsal muscles two simulations were made, with and without the scapular muscles trapezius, levator scapulae, and rhomboideus active. Maximal flexion and extension moments were calculated as the product of the force at the glabella (in extension) and at the ophistocranium (in

flexion) and the orthogonal distance of the force vector to a point in the upper part of the T1 vertebral body (Vasavada et al., 2001), which was fixed in space.

2.5. Segmental instantaneous centres of rotation

Segmental instantaneous centres of rotation (sICR) were evaluated at C7 to Occipital Condyle (OC) level using the method reported by van Mameren et al. (1992), in simulations of physiological flexion and extension according to Appendix B.

2.6. Validation in rear impact

Component level validation of the complete head-neck complex, from T1 and upwards, was made by simulations of rear impact experiments with five female PMHSs reported by Stemper et al. (2003, 2004a, 2004b). In these experiments, specimens were mounted on a mini-sled with an anterior T1 orientation of 25°, the Frankfort plane aligned with the horizontal plane, and the occipital condyles (OCs) aligned superiorly of T1 (Stemper et al., 2003). For the model, the angle of the T1 anterior vertebral body surface was 3° relative to the vertical, Fig. 1 and Table 2. Therefore, it was rotated 22° around the Y-axis during pre-processing for simulation of the experiments. After this rotation, positioning the model with the OCs directly over T1 with a horizontal Frankfort plane was not possible as relatively large elastic forces were created in the ligaments; instead the OCs was positioned approximately 12 mm anterior of T1 and the Frankfort plane angle was adjusted to 6°, Fig. 2, by prescribed rigid body motions 0.1 s prior to the onset of the acceleration pulse, which indicate time zero in the presented results. During the 0.1 s pre-simulation, global damping was used to remove kinetic energy related to the positioning. During all impact simulations, no muscle activation was present.

Two validation simulations were made, one with an acceleration pulse corresponding to a 2.6 m/s velocity change (Stemper et al., 2004b) applied the T1 in the X direction; and a second with a velocity change of 1.3 m/s (Stemper et al., 2003). Model responses were compared with respect to both global head kinematics (Stemper et al. 2004b), which were scaled to correspond to 50th percentile female specimens, Appendix C, and with respect to female specific segmental angulations and facet joint displacements (Stemper et al., 2003) at the time of maximum S-shape, defined as the instant for which the C2C3 segment showed the largest flexion (Stemper et al., 2003).

Table 2
Cervical spine curvature characteristics for the head–neck model in its modelled posture and positioned for the rear impact simulations. OC=Occipital Condyles. T1A=anterior T1 angle.

	Frankfort Plane angle (°)	Anterior T1 angle (°)	OC–T1 X distance (mm)	Curvature index (%)	Superior Bezier angle (°)	Inferior Bezier angle (°)
Modelled posture	11.5	3	–6	0.8	5	7
High T1A, validation simulations	6	25	12	3.5	20	23
Mid T1A	6	14	12	1.7	15	12
Low T1A	6	3	12	0.4	8	0

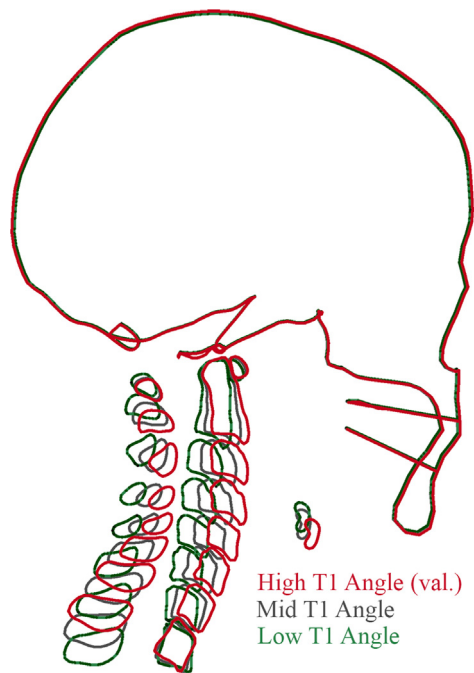


Fig. 2. Schematic cross-section of the skeletal structure in the varied postures for rear end impact simulations in Section 2.7. The High T1 Angle represents the head–neck posture used for the validation (val.) simulations described in Section 2.6.

2.7. The effect of initial spinal curvature in rear impact

A parameter study was conducted to investigate the effect of the initial cervical spinal curvature in a rear impact test (the acceleration pulse of 2.6 m/s according to Section 2.6). The model was rotated around the Y-axis during pre-processing to achieve low (3°) and mid (14°), in addition to the high (25°), anterior T1 angle (T1A) postures, Fig. 2 and Table 2. Then, during the 0.1 s pre-simulation phase the head angle and position was adjusted as described in Section 2.6.

Using the cross-sectional area of each ligament (Östh et al., 2016a) and reported sub-catastrophic and catastrophic failure force levels (Mattucci and Cronin, 2015), corresponding stress levels for each lower cervical spine ligament in the model was calculated, Table D1 in Appendix D. The strain-rate in the impact simulations were on average about 35/s (range 5–85/s) for the ligaments, which is why failure forces reported for a strain rate of 20/s (Mattucci and Cronin, 2015) was used. The stress in the fibre (a-direction) of each element was normalized with the sub-catastrophic and catastrophic stress levels for the ligament to predict injury in the simulated impacts, Figs. D1–4.

3. Results

The female head–neck model consisted of a total of 142,700 elements. A mesh quality assessment (Burkhart et al., 2013) showed that 1% of the elements had an aspect ratio of less than 3 (maximum 10.2), while 97% and 96% of all shell and solid elements had Jacobian values larger than 0.7 (minimum 0.29).

3.1. Spinal alignment assessment

The cervical spine of the model had a curvature index of 0.8%, which together with its superior and inferior Bezier angles,

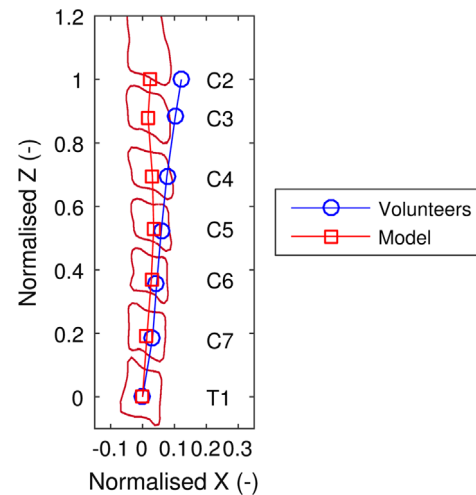


Fig. 3. The spinal alignment of the head–neck model (red squares) is slightly more rearward than the average of the female volunteers (blue circles, Sato et al., 2016). The schematic outline depicts a lateral cross section of the vertebral bodies of the head–neck model in its modelled posture. (For interpretation of the references to color in this figure legend, the reader is referred to the web version of this article.)

Table 2, are at the lower end for human volunteers and would be classified as level 1 mid lordotic (Klinich et al., 2004). The spinal alignment in comparison to the eight female volunteers (Sato et al., 2016), Fig. 3, shows slightly more rearward position of the inferior surface of the C2 vertebral body.

3.2. Maximum strength and segmental instantaneous centres of rotation

The maximal cervical strength of the model was 12.4 Nm in flexion, 31.0 Nm and 42.8 Nm in extension (with and without scapular muscles). This is within the flexion range of 15 Nm (SD 4 Nm) reported for female volunteers by Vasavada et al. (2001), but stronger in than for volunteer extension (mean 21 Nm, SD 12 Nm). In the simulation to evaluate the sICRs, the feedback control was able to create a relatively smooth flexion–extension movement of the cervical spine, Fig. 4, using the models own muscles. The largest contraction was found for the flexor muscles which were activated to 11% during the forward movement. Qualitatively, average sICRs, Fig. 4(b), are similarly located as reported for ten healthy volunteers by van Mameren et al. (1992); the C6C7 and C5C6 sICR are within the intervertebral disc, although at the inferior border. For higher cervical levels, the sICRs are below the intervertebral disc of the segment.

3.3. Validation in rear impact

In the rear impact validation, the overall correlation of the global head kinematics was 0.72 for head rotation and 0.70 for head displacement relative to T1, for the 2.6 m/s simulation, Fig. 5. It appears that the head was lagging slightly more behind than the

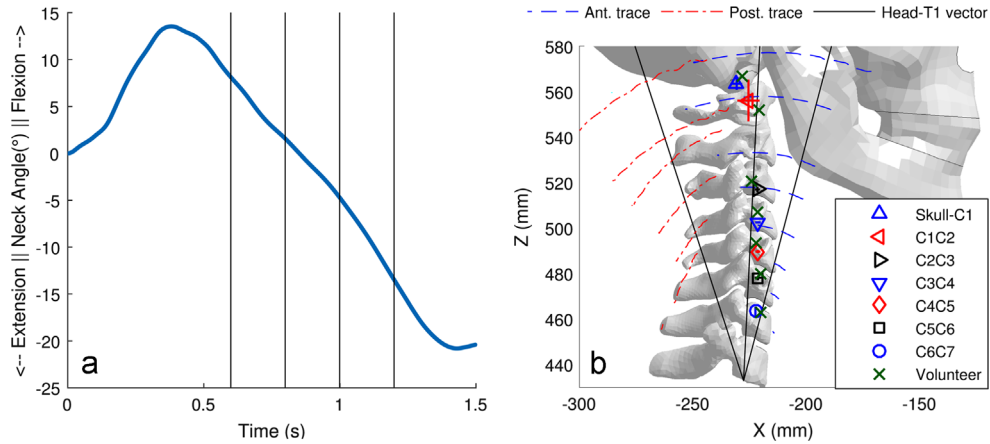


Fig. 4. (a): Change in neck angle, defined as the angle of a vector between T1 and the head centre of gravity, and the vertical axis, in the simulation to determine the Segmental Instantaneous Centres of Rotation (sICR) of the model. Vertical lines indicate time instances at which the sICRs were evaluated. (b): Average sICRs plotted on top of a contour of the model in its initial posture. Markers indicate the average position; the crosshair at each marker the standard deviation in X and Z directions. The volunteer marker data is estimated from van Mameren et al. (1992). The dashed lines indicate the trajectories of the anterior nodes and dash-dotted line of the posterior nodes used for calculating the sICRs. A solid line indicates the head-T1 vector in the initial (middle), most flexed and most extended positions. Ant.=Anterior. Post.=Posterior.

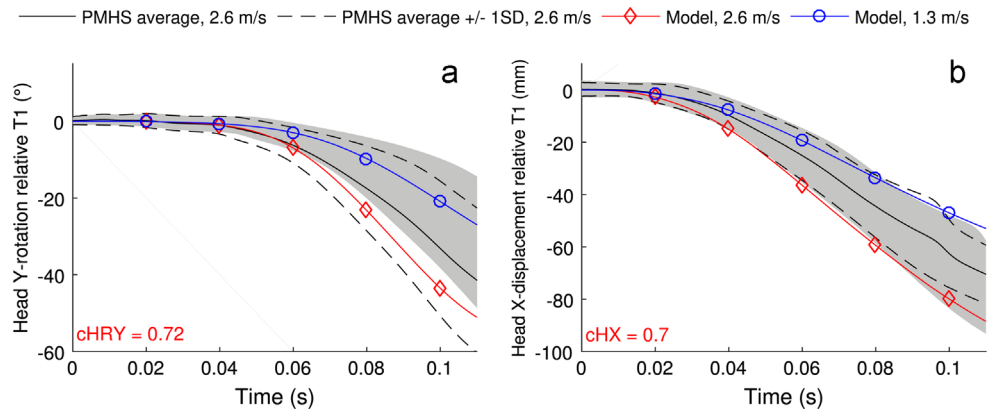


Fig. 5. Global head kinematics of the head-neck model compared with Post Mortem Human Subject (PMHS) corridors in 2.6 m/s impacts (average response \pm 1 Standard Deviation (SD)), in the validation simulation of a 2.6 m/s rear impact. For comparison, the model response in the 1.3 m/s simulation is also included. The PMHS corridors (Stemper et al., 2004b) are scaled to correspond to 50th percentile female responses as described in Appendix C. The light grey shaded area represents the original 50th percentile male corridors (Stemper et al., 2004b). cHRY, cHX=correlation between model response and average PMHS response for Y-rotation (RY) and X displacement at 2.6 m/s.

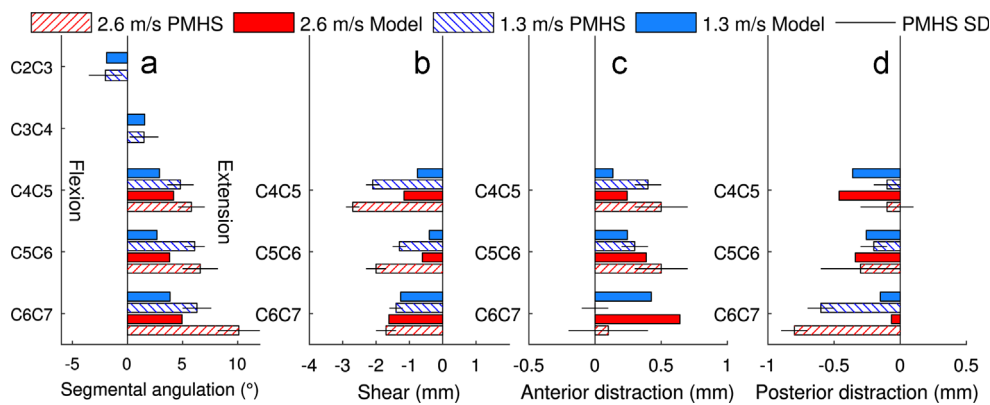


Fig. 6. Segmental angulations and facet joint displacements for the model compared with Post Mortem Human Subject (PMHS) responses (Stemper et al., 2003, 2004a) (average \pm 1 Standard Deviation (SD)), in the validation simulations of 1.3 and 2.6 m/s rear impacts, at the time of peak C2C3 angulation. Facet joint shear is defined as translation of the superior facet relative to the inferior in the plane of the facets. Distraction is the increase in relative distance between inferior and superior nodes on the anterior and posterior end of the facets, in accordance with Stemper et al. (2004a).

average PMHS response; with a stronger coupling to T1 faster head rotation and less relative displacement would occur and these correlations would be higher.

The model showed an S-shaped spine deformation, Fig. 6. The maximum S-shape, occurred at 0.056 s and 0.068 s for the 2.6 m/s

and 1.3 m/s pulse, respectively. This was somewhat earlier compared to the 0.076 and 0.08 s reported for PMHS by Stemper et al. (2003). Here it is worth noting that the experimental average timings also include male subjects, which can be expected to have a slower response due to longer necks.

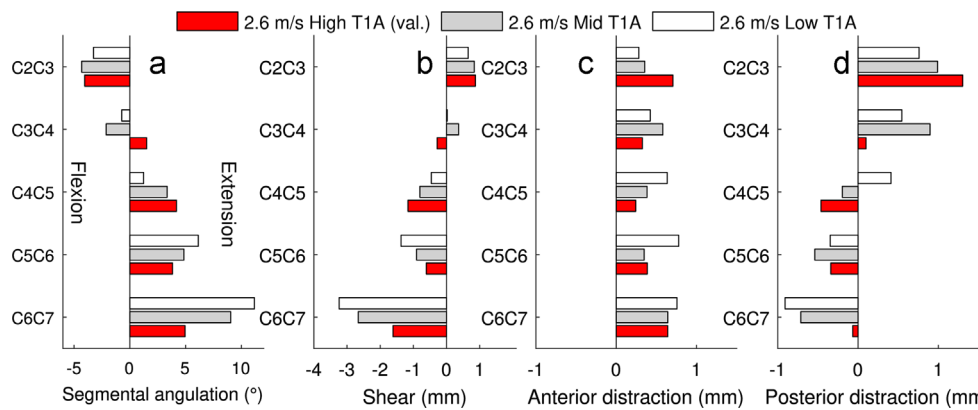


Fig. 7. Segmental angulations and facet joint displacements for all simulations, at the time of peak C2C3 angulation (at 0.056 s, 0.055 s, and 0.058 s respectively). Facet joint shear is defined as translation of the superior facet relative to the inferior in the plane of the facets. Distraction is the increase in relative distance between inferior and superior nodes on the anterior and posterior end of the facets, in accordance with [Stemper et al. \(2004a\)](#). T1A=T1 angle.

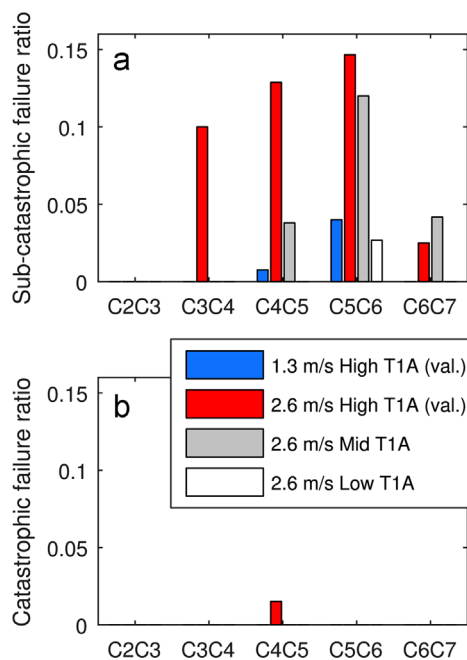


Fig. 8. Ratio of capsular ligament elements which exceeded the sub-catastrophic and catastrophic failure stress levels, [Table D1](#), in the rear impact simulations.

3.4. The effect of initial spinal curvature in rear impact

With a larger anterior T1 angle, a more lordotic shape with a higher curvature index as well as superior and inferior Bezier angles was found, [Table 2](#) and [Fig. 2](#). During impact, normalized ligament stress levels were low for all lower cervical ligaments except the capsular ligaments (CL), which exhibited a peak around the time of the maximum S-Shape, [Figs. D1–D4](#). The altered initial spinal curvature influenced segment level kinematics, [Fig. 7](#), and the number of ligament elements that predicted failure, [Fig. 8](#). The simulation with high T1 angle predicted sub-catastrophic failure in more elements compared to the lower T1 angles, [Fig. 8](#), even though they resulted in more rotation and shear at the C6C7 segment, [Fig. 7](#). Catastrophic failure was only predicted for a few elements in the C4C5 CL for the high T1 angle, [Fig. 8](#).

4. Discussion

A 50th percentile female ligamentous cervical spine was complemented with a rigid body head, soft tissues and Hill-type

muscle elements. For the present study no scaling of the muscle PCSAs were made, as the decline in muscle mass with age appears to be of the same magnitude as the difference between adult females and males ([Marras et al., 2001](#); [Van Ee et al., 2000](#)). The extension strength of the model when including the scapular muscles was too large compared with female volunteers ([Vasavada et al., 2001](#)). The scapular muscle contribute to isometric cervical extension ([Blouin et al., 2007](#)), but might not be fully active as in the present simulations as their main physiological function is elevation of the scapula ([Standring, 2008](#)). The scapular muscles contribute less to dynamic motions ([Ólafsdóttir et al., 2015](#)), such as rear impact. In physiological motions, actuated by its own muscles and with gravity load, the model's sICRs were qualitatively in agreement with that of healthy human volunteers ([van Mameren et al., 1992](#)).

The majority of both males and females had a mid lordotic cervical spine ([Klinich et al., 2004](#)) just as the developed model; its curvature index, [Table 2](#), is within the range for young subjects, while it compares better with tall (> 163 cm) than mid-size females ([Klinich et al., 2004](#)). To position the model for the validation simulation, the T1 angle was increased to 25°, while the head was allowed to be slightly more forward and rotated upward than specified in the corresponding PMHS study ([Stemper et al., 2003](#); [2004a](#)). The initial curvature of the cervical spine has an influence on the segment level kinematics, [Fig. 7](#), and on the stress of the CL during impact, [Fig. 8](#). For a higher T1 angle less extension and shear of the lower segments was found, [Fig. 7](#), but a higher ratio of CL elements exceeded the sub-catastrophic failure stress, [Fig. 8](#). This was likely because positioning the model into a lordotic shape pre-strains the ligaments. Sub-catastrophic failure of CL ligaments is one possible cause of long-term WAD ([Bogduk, 2011](#)), which is why a higher ratio of failed elements for the model is likely to correlate with a higher risk for WAD. No significant stress levels were generated due to the positioning, [Figs. D1–D4](#), showing that all simulated postures were achievable by motions within the neutral zone ([Panjabi et al., 2001](#)) of each segment.

Similar to the present work, [Stemper et al. \(2005\)](#) validated a male head–neck model and studied the influence of cervical curvature, for a lordotic, straight, and kyphotic posture. They reported increased CL elongation for the kyphotic posture in comparison with the lordotic, and concluded that such an abnormal posture can contribute to an increased risk of WAD in a rear impact. [Stemper et al. \(2005\)](#) adjusted initial ligament lengths for each posture simulated; hence, their models represent individuals whose cervical spine neutral position are lordotic, straight, or kyphotic. In the present work, the female model was positioned during simulation without adjustment of initial ligament lengths,

thereby representing one individual maintaining the same head position with different initial spinal curvatures. The more lordotic (the high and mid T1 angle) postures predicted a higher risk of injury as more elements exceeded the sub-catastrophic failure level during impact. *Sato et al. (2016)* recently showed that male and female volunteers exhibit different spinal alignment in the same seat. In the light of the results of the present study, one can speculate that automotive seat geometry leads to females assuming a cervical spine alignment with more pre-strain of the CL relative to their neutral posture, and this could be a contribution to the higher risk of WAD for females compared with males.

In the present study, the rear impact simulations were run without any muscle activation, as the model was compared with the response of PMHSs. The passive elastic stiffness of the muscles provided low forces, less than 0.5 N. For future studies, reflexive muscle responses will be incorporated in the model using a feedback control approach (*Östh et al., 2012*), to enable comparisons to female volunteers in rear impacts. The kinematic whole body model that is currently under development will be merged with the female cervical spine model presented here, and will be used for injury reconstruction of rear impacts. Thereby, in order to provide a tool that can be used to develop automotive protective systems for the group of vehicle occupants which are at the greatest risk of sustaining WAD, we can create model specific injury risk functions for WAD for females in rear impacts.

Conflict of interest

The authors have no conflicts of interest.

Acknowledgements

This study was funded by VINNOVA – Swedish Governmental Agency for Innovation Systems (grant no. 2013–03095), carried out at SAFER–Vehicle and Traffic Safety Centre at Chalmers, and simulations were performed on resources at Chalmers Centre for Computational Science and Engineering (C3SE) provided by the Swedish National Infrastructure for Computing (SNIC). The authors acknowledge Elemance, LLC. (Winston-Salem, NC) for STL surface geometry development in support of this project. Lastly, the authors would like to thank Elisabet Agar for language editing of the manuscript.

Appendices. Supplementary material

Supplementary data associated with this article can be found in the online version at <http://dx.doi.org/10.1016/j.jbiomech.2016.11.066>.

References

- Beier, G., Schuller, E., Schuck, M., Ewing, C.L., Becker, E.D., Thomas, D.J., 1980. Center of gravity and moments of inertia of human heads. In: Proceedings of the IRCOBI Conference, Birmingham, England. pp. 218–228.
- Blouin, J.-S., Siegmund, G.P., Carpenter, M.G., Inglis, J.T., 2007. Neural control of superficial and deep neck muscles in humans. *J. Neurophysiol.* 98, 920–928.
- Bogduk, N., 2011. On cervical zygapophysial joint pain after whiplash. *Spine* 36 (25S), S194–S199.
- Borst, J., Forbes, P.A., Happee, R., Veeger, H.E.J., 2011. Muscle parameters for musculoskeletal modelling of the human neck. *Clin. Biomech.* 26, 343–351.
- Brolin, K., Östh, J., Svensson, M., Sato, F., Ono, K., Linder, A., Kullgren, A., 2015. Aiming for an average female virtual human body model for seat performance assessment in rear-end impacts. In: Proceedings of the 24th ESV Conference, Paper no. 15-0247.
- Burdett, E., Mitchell, V., 2008. Anatomy of the larynx, trachea and bronchii. *Anaesth. Intensive Care* 9 (8), 329–333.
- Burkhart, T.A., Andrews, D.M., Dunning, C.E., 2013. Finite element mesh quality, energy balance and validation methods: a review with recommendations associated with the modeling of bone tissue. *J. Biomech.* 46, 1477–1488.
- Carlsson, A., Chang, F., Lemmen, P., Kullgren, A., Schmitt, K.-U., Linder, A., Svensson, M.Y., 2014. Anthropometric specifications, development, and evaluation of EvaRID – A 50th percentile female rear impact finite element dummy model. *Traffic Inj. Prev.* 15, 855–865.
- Carstensen, T.B., Frostholm, L., Oernboel, E., Kongsted, A., Kasch, H., Jensen, T.S., Fink, P., 2012. Are there gender differences in coping with neck pain following acute whiplash trauma? A 12-month follow-up study. *Eur. J. Pain.* 16, 49–60.
- Cole, G.K., van den Bogert, A.J., Herzog, W., Gerritsen, K.G., 1996. Modelling of force production in skeletal muscle undergoing stretch. *J. Biomech.* 29 (8), 1091–1104.
- de Bruijn, E., van der Helm, F.C.T., Happee, R., 2015. Analysis of isometric cervical strength with a non-linear musculoskeletal model with 48 degrees of freedom. *Multibody Syst. Dyn.* 34 (4), 339–362.
- de Jager, M.K.J., 1996. Mathematical head-neck models for acceleration impacts (PhD. thesis). Eindhoven University of Technology, Eindhoven, The Netherlands.
- Ejima, S., Ono, K., Kaneoka, K., Fukushima, M., 2005. Development and validation of the human neck muscle model under impact loading. In: Proceedings of the IRCOBI Conference, Prague, Czech Republic. pp. 245–255.
- Engelbrektsson, K., 2011. Evaluation of material models in LS-DYNA for impact simulation of white adipose tissue. MSc. Thesis. Chalmers University of Technology, Gothenburg, Sweden.
- Gayzik, F.S., Hamilton, C.A., Tan, J.C., McNally, C., Duma, S.M., Klinich, K.D., Stitzel, J.D., 2009. A multi-modality image data collection protocol for full body finite element model development. SAE Technical Paper 2009-01-2261. SAE International, Warrendale, PA, USA.
- Gayzik, F.S., Moreno, D.P., Geer, C.P., Wuertzler, S.D., Martin, R.S., Stitzel, J.D., 2011. Development of a full body CAD dataset for computational modeling: a multi-modality approach. *Ann. Biomed. Eng.* 39 (10), 2568–2583.
- Gordon, C.T., Churchill, T., Clauser, C.E., Brandtmiller, B., McConville, J.T., Tebbetts, I., Walker, R.A., 1989. 1988 Anthropometric survey of U.S. army personnel: methods and summary statistics. United States Army Natick Research Development and Engineering Center, Natick, MA.
- Halldin, P., Brolin, K., Kleiven, S., von Holst, H., Jakobsson, L., Palmertz, C., 2000. Investigation of conditions that affect neck compression-flexion injuries using numerical techniques. In: Proceedings of the 44th Stapp Car Crash Conference, Atlanta, GA, USA. Paper no. 2001-01-SC10.
- Hovenga, P.E., Spit, H.H., Uijldert, M., Dalenoort, A.M., 2005. Improved prediction of Hybrid-III injury values using advanced multibody techniques and objective rating. SAE Technical Paper 2005-01-1307. SAE International, Warrendale, PA, USA.
- Jakobsson, L., Norin, H., Svensson, M.Y., 2004. Parameters influencing AIS 1 neck injury outcome in frontal impacts. *Traffic Inj. Prev.* 5, 156–163.
- Kamibayashi, L.K., Richmond, F.J.R., 1998. Morphometry of human neck muscles. *Spine* 23 (12), 1314–1323.
- Kaneoka, K., Ono, K., Inami, S., Koichiro, H., 1999. Motion analysis of cervical vertebrae during whiplash loading. *Spine* 24 (8), 763–769.
- Karmakar, A., Pate, M.B., Solowski, N.L., Postma, G.N., Weinberger, P.M., 2014. Tracheal size variability is associated with sex: implications for endotracheal tube selection. *Ann. Otol. Rhinol. Laryngol.* <http://dx.doi.org/10.1177/0003489414549154>
- Kitagawa, Y., Yasuki, T., Hasegawa, J., 2008. Research study on neck injury lessening with active head restraint using human body FE model. *Traffic Inj. Prev.* 9 (6), 574–582.
- Klinich, K., Ebert, S.M., Van, Ee, C.A., Flannagan, C.A., Prasad, M., Reed, M.P., Schneider, L.W., 2004. Cervical spine geometry in the automotive seated posture: variations with age, stature, and gender. *Stapp Car Crash J.*, 48.
- Krafft, M., Kullgren, A., Lie, A., Tingvall, C., 2003. The risk of whiplash injury in the rear seat compared to the front seat in rear impacts. *Traffic Inj. Prev.* 4, 136–140.
- Kullgren, A., Krafft, M., Lie, A., Tingvall, C., 2007. The effect of whiplash protection systems in real-life crashes and their correlation to consumer crash test programmes. In: Proceedings of the 20th ESV Conference.
- Manschot, J.E.M., Brakkee, A.J.M., 1986. The measurement and modelling of the mechanical properties of human skin in vivo – II. The model. *J. Biomech.* 19 (7), 517–521.
- Marras, W.S., Jorgensen, M.J., Granat, K.P., Wiand, B., 2001. Female and male trunk geometry: size and prediction of the spine loading trunk muscles derived from MRI. *Clin. Biomech.* 16, 38–46.
- Mattucci, S.F.E., Cronin, D.S., 2015. A method to characterize average cervical spine ligament response based on raw data sets for implementation into injury biomechanics models. *J. Mech. Behav. Biomed. Mater.* 41, 251–260.
- Mordaka, J., 2004. Finite element analysis of whiplash injury for women (PhD. thesis). Nottingham Trent University, Nottingham, UK.
- Morris, A.P., Thomas, P.D., 1996. Neck injuries in the UK co-operative crash injury study. In: Proceedings of the 40th Stapp Car Crash Conference. pp. 317–329.
- Mustafay, T., El-Rich, M., Mesfar, W., Moglo, K., 2014. Investigation of impact loading rate effects on the ligamentous cervical spine load-partitioning using finite element model of functional unit C2–C3. *J. Biomech.* 47, 2891–2903.
- Nightingale, R.W., Sganga, J., Cutcliffe, H., Bass, C.R., 2016. Impact responses of the cervical spine: a computational study of the effects of muscle activity, torso constraint, and pre-flexion. *J. Biomech.* 49, 558–564.

- Ólafsdóttir, J.M., Brolin, K., Blouin, J.-S., Siegmund, G.P., 2015. Dynamic spatial tuning of cervical muscle reflexes to multidirectional seated perturbations. *Spine* 40 (4), E2211–E2219.
- O'Neill, B., Haddon Jr, W., Kelley, A.B., Sorenson, W.W., 1972. Automobile head restraints: frequency of neck injury claims in relation to the presence of head restraints. *Am. J. Public Health* 62, 309–406.
- Östh, J., Brolin, K., Carlsson, S., Wismans, J., Davidsson, J., 2012. The occupant response to autonomous braking: a modeling approach that accounts for active musculature. *Traffic Inj. Prev.* 13 (3), 265–277.
- Östh, J., Brolin, K., Svensson, M.Y., Linder, A., 2016a. A female ligamentous cervical spine finite element model validated for physiological loading. *J. Biomech. Eng.* 138 (6).
- Östh, J., Mendoza-Vazquez, M., Svensson, M.Y., Linder, A., Brolin, K., 2016b. Development of a 50th percentile female human body model. In: Proceedings of the IRCOBI Conference, Malaga, Spain.
- Panjabi, M.M., Crisco, J.J., Vasavada, A., Oda, T., Cholewicki, J., Nibu, K., Shin, E., 2001. Mechanical properties of the human cervical spine as shown by three-dimensional load-displacement curves. *Spine* 26, 2692–2700.
- Panzer, M., Cronin, D., 2009. C4–C5 segment finite element model development, validation, and load-sharing investigation. *J. Biomech.* 42, 480–490.
- Plaga, J.A., Albery, C., Boehmer, M., Goodyear, C., Thomas, G., 2005. Design and development of anthropometrically correct head forms for Joints Strike Fighter ejection seat testing. AFRL-HE-WP-TR-2005-0044, Air Force Research Laboratory. Wright-Patterson Air Force Base, USA.
- Roberts, C.R., Rains, J.K., Paré, P.D., Walker, D.C., Wiggs, B., Bert, J.L., 1998. Ultrastructure and tensile properties of human tracheal cartilage. *J. Biomech.* 31, 81–86.
- Sato, F., Odani, M., Miyazaki, Y., Yamazaki, K., Östh, J., Svensson, M.Y., 2016. Effects of whole spine alignment patterns on neck responses in rear end impact. *Traffic Inj. Prev.* <http://dx.doi.org/10.1080/15389588.2016.1227072>
- Schneider, L.W., Robbins, D.H., Pflüg, M.A., Snyder, R.G., 1983. Development of anthropometrically based design specifications for an advanced adult anthropomorphic dummy family (Final Report). University of Michigan Transportation Research Institute, Ann Arbor, MI.
- Standring, S. (Ed.), 2008. *Gray's Anatomy – The anatomical basis of clinical practice*. Elsevier Churchill Livingstone, London, UK.
- Stemper, B.D., Pintar, F.A., Rao, R.D., 2011. The influence of morphology on cervical injury characteristics. *Spine* 36 (25S), S180–S186.
- Stemper, B.D., Yoganandan, N., Pintar, F.A., 2003. Gender dependent cervical spine segmental kinematics during whiplash. *J. Biomech.* 36, 1281–1289.
- Stemper, B.D., Yoganandan, N., Pintar, F.A., 2004a. Gender- and region-dependent local facet joint kinematics in rear impact. *Spine* 29, 1764–1771.
- Stemper, B.D., Yoganandan, N., Pintar, F.A., 2004b. Response corridors of the human head-neck complex in rear impact. In: 48th Annual Proceedings of the Association for the Advancement of Automotive Medicine.
- Stemper, B.D., Yoganandan, N., Pintar, F.A., 2005. Effects of abnormal posture on capsular ligament elongations in a computational model subjected to whiplash loading. *J. Biomech.* 38, 1313–1323.
- Stigson, H., Gustafsson, M., Sunnevång, C., Krafft, M., Kullgren, A., 2015. Differences in long-term medical consequences depending on impact direction involving passenger cars. *Traffic Inj. Prev.* 16, S133–S139.
- Temming, J., Zobel, R., 1998. Frequency and risk of cervical spine distortion injuries in passenger car accidents: significance of human factors data. In: Proceedings of the IRCOBI Conference, pp. 219–233.
- van der Horst, M., 2002. *Human Head Neck Response in Frontal, Lateral and Rear End Impact Loading – Modeling and Validation* (PhD. Thesis). Eindhoven University of Technology, Eindhoven, the Netherlands.
- VanE.A., Nightingale, R.W., Camacho, D.L.A., Chancy, V.C., Knaub, K.E., Sun, E.A., Myers, B.S., 2000. Tensile properties of the human muscular and ligamentous cervical spine. In: Proceedings of the 44th Stapp Car Crash Conference.
- Van Mameren, H., Sanches, H., Beursgens, J., Drukker, J., 1992. Cervical spine motion in the sagittal plane II: position of segmental averaged instantaneous centers of rotation—a cineradiographic study. *Spine* 17 (5), 467–474.
- Vasavada, A.N., Danaraj, J., Siegmund, G.P., 2008. Head and neck anthropometry, vertebral geometry and neck strength in height-matched men and women. *J. Biomech.* 41, 114–121.
- Vasavada, A.N., Li, S., Delp, S.L., 2001. Three-dimensional isometric strength of neck muscles in humans. *Spine* 26 (17), 1904–1909.
- Walker, S.M., Schrodt, G.R., 1974. Segment lengths and thin filament periods in skeletal muscle fibers of the rhesus monkey and the human. *Anat. Rec.* 178, 63–82.
- Watanabe, Y., Ichikawa, H., Kayama, O., Ono, K., Kaneoka, K., Inami, S., 2000. Influence of seat characteristics on occupant motion in low-velocity rear-end impacts. *Accid. Anal. Prev.* 32, 243–250.
- Winters, J.M., Stark, L., 1988. Estimated mechanical properties of synergistic muscles involved in movements of a variety of human joints. *J. Biomech.* 21 (12), 1027–1041.
- Yamada, H., 1970. *Strength of Biological Materials*. Williams & Wilkins, Baltimore, MD.
- Yang, K., Zhu, F., Luan, F., Zhao, L., Begeman, P., 1998. Development of a finite element model of the human neck. In: Proceedings of the 42nd Stapp Car Crash Conference, Tempe, AZ, USA. Paper no. 983157.
- Yoganandan, N., Pintar, F., Zhang, J., Baisden, J.L., 2009. Physical properties of the human head: mass, Center of Gravity, and Moment of Inertia. *J. Biomech.* 42 (9), 1177–1192.
- Yoganandan, N., Pintar, F.A., Stemper, B.D., Schlick, M.B., Philippens, M., Wismans, J., 2000. Biomechanics of human occupants in simulated rear crashes: documentation of neck injuries and comparison of neck injury criteria. *Stapp Car Crash J.* 44, 189–204.
- Zajac, F.E., 1989. Muscle and tendon: properties, models, scaling, and application to biomechanics and motor control. *Crit. Rev. Biomed. Eng.* 17 (4), 359–411.